Cell tracking with ^{19}F MRI

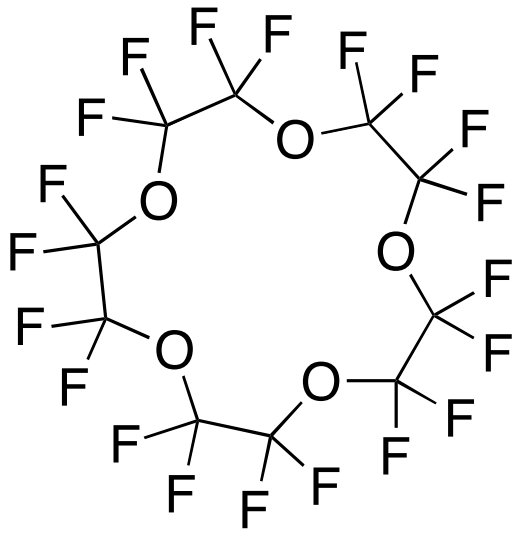

S.F. Oppedijk
Student number: 3116468

Drug Innovation – Literature Thesis

Image Science Institute – In vivo NMR
Supervisor: Dr. G. van Tilborg

21 September 2012

Illustration:
Perfluoro-5-crown-ether: one of the most frequently uses perfluorocarbons in ^{19}F MRI

1. Table of contents

2. List of abbreviations

Å	angstrom (10^{-10})
BMDC	bone marrow derived dendritic cell
cryoTEM	cryo-transmission electron microscopy
DC	dendritic cell
DIC microscopy	Differential interference contrast microscopy
ECG	Electrocardiagram
FACS	Fluorescence-activated cell sorting
FBPA	Fluorescent blended PFPE amides
FDA	Food and Drug administration, USA
FSDC	Fetal skin derived dendritic cell
FSE	Fast spin echo
kg	kilogram
L	liter
mL	mililiter
mM	milimolar
MR	magnetic resonance
MRI	magnetic resonance imaging
MRS	magnetic resonance spectroscopy
MSPIO	Micron sized paramagnetic iron oxide
NAO assay	nonyl acridine orange assay
nm	nanometer
NMR	nuclear magnetic resonance
NPC	neural progenitor cells
NSC	neural stem cells
PCE	perfluoro-15-crown-5-ether
PCS	photon correlation spectroscopy
PFC	perfluorocarbon
PFOB	perfluorooctyl bromide
PFPE	perfluoropolyether
PMA	Phorbol-12-myristate-13-acetate
pmol	picomole
PSI	Pound per square inch
RARE	Relaxation
RES	reticuloendothelial system
RF	resonance freqency
rpm	rounds per minute
SNR	signal-to-noise ratio
SPIO	small paramagnetic iron oxide
T	Tesla
TFA	trifluoroacetic acid
USPIO	ultrasmallparamagnetic iron oxide
VCAM-1	vascular cellular adhesion molecule 1
µm	micrometer

3. Introduction on a new type of compound: perfluorocarbons

Perfluorocarbons (PFCs) are carbon-based compounds derived from hydrocarbons that have their hydrogen atoms completely substituted with fluorine. PFCs have already been widely tested, evaluated and used in biological applications, as they are considered a promising class of compounds serving as an oxygen carrier in the blood.[1] The commercially available PFC nanoemulsion Oxygent™ has been clinically tested in a phase III clinical trial in humans for the treatment of respiratory distress syndrome during surgeries.[2, 3] The PFCs were applied while saturated with oxygen to enhance the oxygen delivery and improve the oxygenation in tissue and it was proven that the use of PFCs allowed minimization of red blood cell transfusion.[2, 4] However, due to an inappropriate testing protocol during the phase III clinical trial and a subsequent lack of funding the use of these particles was never further developed.
PFCs are considered valuable compounds for medical applications because of their high stability and incredible chemical and biological inertness.[1, 2, 4-9] In the past years PFCs have been tested mainly in therapeutic application. The ability to track the behavior of (therapeutic) cells and (fluorine containing) drugs in a non-invasive way *in vivo* will provide clinicians with valuable information on the accumulation of these cells or compounds.[6, 10-12] One important example of such cells are immune cells, which specifically accumulate sites of inflammation. Labeling of leukocytes, such as monocytes and T-cells, with fluorine containing emulsions provides the possibility to image these cells *in vivo* at sites of inflammation.[3, 5, 6, 9-11, 13-44] This thesis will provide an overview of the research conducted on imaging of inflammation with ^{19}F MR Imaging using PFCs as a tracer.

3.1 Physicochemical properties

The fluorine atom is larger than the hydrogen atom with an estimated Van der Waals radius of 1.47 Å compared to 1.20 Å for hydrogen.[8, 45, 46] As a consequence of the slightly larger Van der Waals radius the rotation around the C-C bond in perfluorocarbons is more restricted than for hydrocarbons, resulting in a more rigid structure.[4] Another consequence is that PFCs are more bulky than regular alkyl chains and tend to have a more helical structure as also illustrated in figure 1.[8, 26]

Fluorine is the most electronegative atom in the periodic table. It has very dense electron clouds resulting in low polarizability and low intermolecular cohesion.[1, 4, 6] Kinetically, the C-F bond is really strong, due to a most favored overlap of the atomic orbitals of carbon and fluorine. This results in the strongest covalent single bond found in molecules.[4] Due to these properties perfluorocarbons differ significantly from hydrocarbons in their stability, fluidity and dielectric constants.[4, 5, 8] Perfluorocarbons are both hydrophobic and lipophobic, which provides the driving force for perfluorocarbons to spontaneously form stable and well-organized bilayers and films.[5, 8]

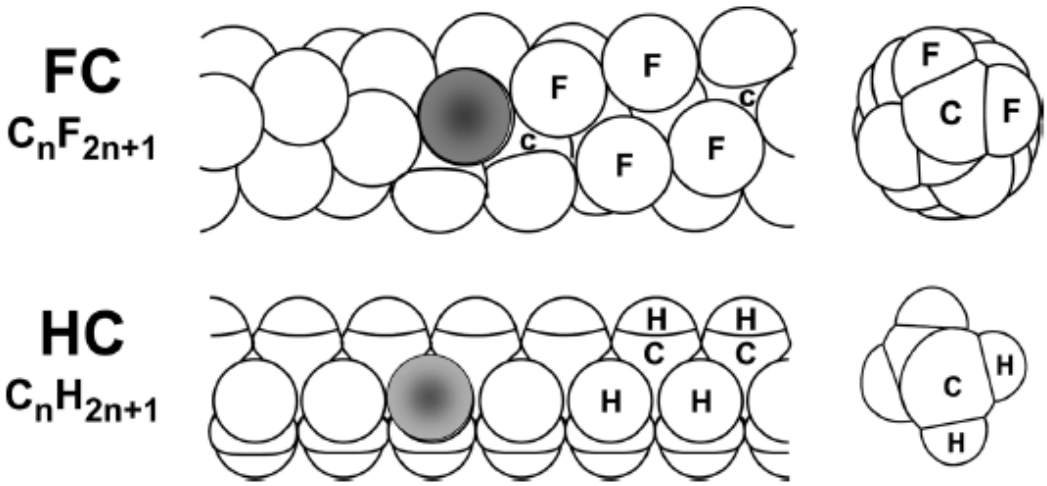

Figure 1: Structure of hydrocarbons versus perfluorocarbons. Perfluorocarbons have a more bulkier structure due to their slightly larger Van der Waals radius compared to hydrogen. Figure taken from Riess.[4]

In very nonpolar solvents the only forces keeping molecules together are the Van der Waals interactions between molecules. The low Van der Waals interactions between perfluorocarbons make them behave as nearly ideal, gas-like fluids, which is also the nature of their ability to dissolve large amounts of gasses.[1, 4, 6, 8] Due to the strong intra-molecular bonds and their lipo- and hydrophobicity perfluorocarbons are extremely stable, show high chemical and biological inertness and do not seem to overt toxicity even at very high concentrations.[1, 2, 4-8, 23, 33, 37] Therefore these kinds of compounds have already been widely tested for several medical purposes, including their use as blood supplements, artificial oxygen carriers,[1, 2] drug delivery systems[3] and microbubbles.[35, 47]
The hydro- and lipophobic character of perfluorocarbons requires formulation into stable emulsions in order to be useful in biological applications.[9] The preparation of these nanoemulsions is described in chapter 5.3.

3.2 Usage and safety profile

Due to their hydro- and lipophobic character PFCs do not incorporate into cell membranes or enter cells without being formulated in biocompatible nanoemulsions.[6] Two of these nanoemulsions, i.e. Oxygent™ (Perflubron, perfluorooctylbromide) and Oxyfluor (Perfluorodichloroctane), have been preclinically tested for intravenious administration to rodents. Oxygent™ was even used in a phase III clinical trial in humans.[2, 3] Before approval for (pre)-clinical testing, these formulations underwent extensive safety testing.[42] These results formed the basis for approval of the start of the clinical trials, but unfortunately none of these results are published in scientific literature.[2] Common side effects accompanied with the use of PFCs are flu-like,[2, 48] possibly caused by the release of cytokines.[48] These symptoms can be related to normal phagocytic activity and the magnitude of the effects is dependent on particle size.[2, 42]

3.3 Biodistribution of perfluorocarbons

The intravascular half-life for Oxygent™ was determined to be 9.4±2.2h for a dose of 1.8g/kg.[2] From the tissue samples collected by Mattrey *et al.* the half-life of perfluorooctylbromide (PFOB) was determined to be approximately 5 days in the liver.[49] For other PFCs, including perfluoro-15-crown-5-ether (PCE) and perfluoropolyether (PFPE), their resonance frequencies could still be observed after 14 days.[15, 29]

Accumulation of PFCs is observed in cells of the reticuloendothelial system (RES). After uptake by these cells, PFC droplets are broken down into individual PFC molecules, which diffuse back into the blood. In the blood they are subsequently transported to the lungs, liver and spleen.[14, 18, 35] Excretion of the PFCs occurs via the lungs and the skin as a vapor[2, 26, 49]

Up to now there are no human enzymes and pathways known for the degradation of individual PFC molecules *in vivo*[2, 6, 24, 36] and they are found to be stable at lysosomal pH.[6, 11] After intravenous administration of a PFC nanoemulsion the nanodroplets are selectively taken up by monocytes and macrophages of the reticuloendothelial system (RES). In case of inflammation, PFC-labeled monocytes and macrophages may accumulate in those areas thereby providing positive signals at sites of inflammation.[2, 6, 48, 50]

4. NMR, MRI and contrast agents

4.1 Introduction on NMR

Nuclear Magnetic Resonance (NMR) is the basis of MRI and is a valuable tool for resolving chemical structure. NMR can only be conducted on nuclei that have a nuclear spin of >1/2. In NMR and MRI the natural abundance and sensitivity of isotopes that contain a natural nuclear spin is very important. The most commonly used nuclei in magnetic resonance (MR) are ^{1}H and ^{13}C. Unfortunately, the ^{12}C isotope of carbon is more abundant than its MR active counterpart. Other isotopes containing a nuclear spin used in MR are ^{14}N, ^{31}P, ^{23}Na, ^{39}K, ^{17}O and ^{19}F. [51, 52]

Table 1: Properties of some commonly used nuclei. Taken from Wechselberger.[52]

Isotope	Nuclear spin I	Resonance frequency (MHz)*	Gyro magnetic ratio γ (T^{-1} s^{-1})	Natural abundance (%)
^{1}H	½	600.0	2.6752×10^{8}	99.985
^{2}H	1	92.1	4.1065×10^{7}	0.015
^{12}C	0	-	-	98.89
^{13}C	½	150.9	6.7266×10^{7}	1.11
^{14}N	1	43.3	1.9325×10^{7}	99.63
^{15}N	½	60.8	-2.7108×10^{7}	0.37
^{16}O	0	-	-	99.76
^{17}O	5/2	81.4	-3.6267×10^{7}	0.04
^{19}F	½	564.5	2.5167×10^{8}	100.0
^{31}P	½	242.9	1.0829×10^{8}	100.0

* Resonance frequency at a magnetic field of 14.092T.

The Larmor frequency provides a measure for the ease of an atom's spin to be influenced by an external magnetic field. This property is only dependent on the gyromagnetic ratio of the atom, i.e. the relation between the magnetic dipole moment to its angular momentum, and the applied magnetic field. On atoms without a nuclear spin an external applied magnetic field will have no influence. If the Larmor frequency would be the same for all proton nuclei, NMR would not be able to distinguish between atoms. Fortunately spins in the same types of atoms do have slightly different Larmor frequencies. These are caused by differences in electron densities, which depend on chemical bonds, resulting in a change in the effective shielding of the electron clouds surrounding the atom's nucleus. A hydrogen atom will have a slightly lower Larmor frequency when it is located next to an electron withdrawing oxygen atom because the electrons surrounding its nucleus will be located relatively closer to the oxygen. In this example, the influence of the magnetic field on the hydrogen nucleus will be greater for the hydrogen closer to the oxygen, resulting in a difference in resonance frequency between the two hydrogen atoms. Therefore, NMR is a useful tool in chemical structure resolution. Additionally, individual spins in close proximity can also influence each other resulting in pattern splitting of the

signal. The size of the coupling between two or more protons is expressed in J-coupling (Hz) and provides valuable information on conformation and the amount of neighboring protons. Figure 2 for example shows the structure of methyl ethanoate. The three red protons give a signal in the shape of a triplet due to the coupling with their two neighbors. The middle signal is the chemical shift of the protons if they would not have any other protons on neighboring carbons. The two adjacent signals are due to coupling with each of the two neighboring protons. The same holds for the green protons, they get influenced by three neighboring protons resulting in a signal splitting into a quartet. Figure 3 shows the structure of crown-5-ether where all the protons are equivalent, and therefore demonstrate a single resonance frequency in the NMR spectrum.[53]

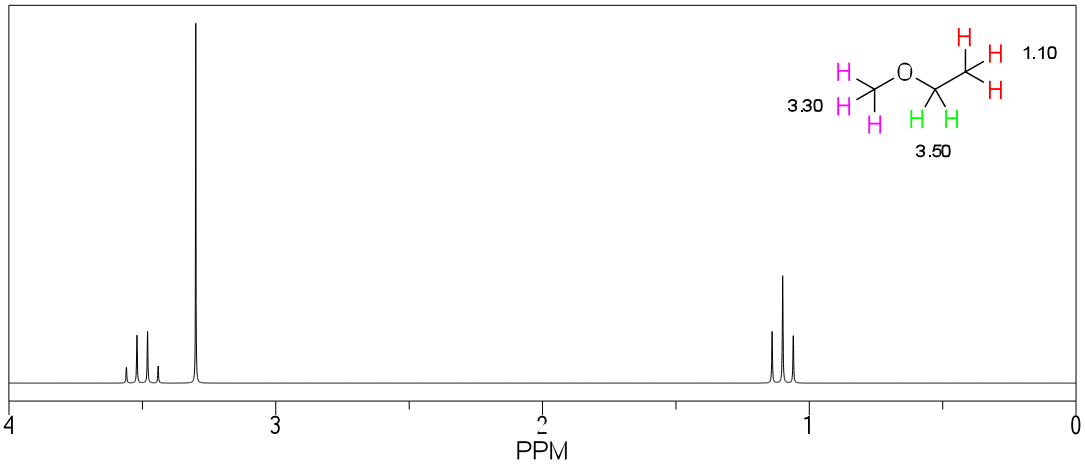

Figure 2: NMR spectrum from methyl ethanoate.
The chemical shifts (ppm) are given for all protons. All protons shown in the same color are chemically equivalent. The protons shown in red are influenced by J-coupling with the protons shown in green resulting in signal splitting in a triplet. The same J-coupling is influencing the signal pattern of the protons expressed in green. The signal is split into a quartet due to the coupling with 3 other protons. The protons shown in pink are not in close proximity to other magnetic spins resulting in a single resonance frequency. The spectrum was simulated and taken from CS Chemdraw Ultra.[53]

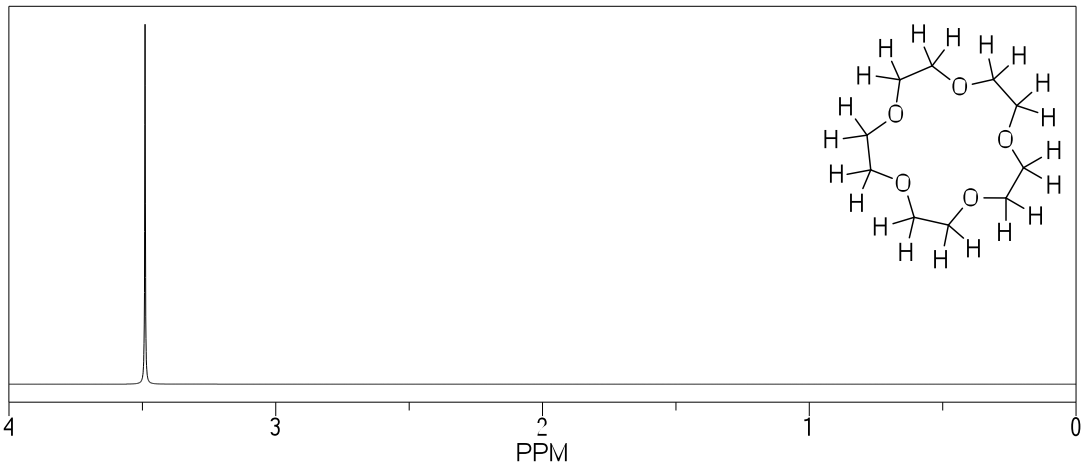

Figure 3: NMR spectrum of crown-5-ether.
In crown-5-ether all protons are chemically equivalent. Due to the high symmetry of the molecule the J-coupling between neighboring protons is canceled out resulting in only one single resonance frequency. The spectrum was simulated and taken from CS Chemdraw Ultra.[53]

The integration of the signals in a NMR spectrum is a measure for the amount of nuclei. Therefore direct quantification of concentration is possible when using a reference sample. The nature of ^{1}H NMR and ^{19}F NMR is the same. Chemical shifts of individual PFCs do not alter when they are formulated into nanoemulsions or incorporated into cells.[6]

4.2 The use of contrast agents in MRI

The use of NMR for imaging purposes is called Magnetic Resonance Imaging (MRI). MRI is a non-invasive imaging technique that makes use of the magnetic resonance frequency of protons in water molecules. The density of water and the rate of relaxation in different types of tissue enables the generation of contrast in MRI. Without MRI the monitoring cells is often conducted with histological tests, for which animals are sacrificed or tissue biopsies are taken. MRI provides the ability to track cells in a non-invasive way *in vivo*.[14]
Many laboratories have attempted to visualize (immune) cells by the use of conventional ^{1}H MRI. For this purpose, cells are labeled with contrast agents in order to provide additional/exogenous contrast in the MRI images. Such contrast agents include paramagnetic particles, composed of iron oxide crystals, or other paramagnetic agents like gadolinium containing particles. This approach has already been widely used in many studies to label and track cells.[6, 10, 15, 20-22] The labels used for MRI cell tracking are briefly described in the following paragraphs.

4.2.1 Iron oxide based (USPIO/SPIO/MPIO)

Iron oxide particles provide contrast in a MR image by locally disrupting the magnetic field, resulting in dark spots (hypointensities) in the image.[15, 20] SPIOs (Super Paramagnetic Iron Oxide particles), USPIOs (Ultrasmall Super Paramagnetic Iron Oxide particles) and MPIOs (Micron Iron Oxide particles) differ in size, and all of them predominantly influence T_2/T_2^* relaxation times of the surrounding protons in water molecules.[6] The particles contain Fe^{2+} and Fe^{3+} ions caught up in a crystal lattice giving them a large magnetic moment.[20]
Cell detection using iron oxide agents can be extremely sensitive and detection of single cells has been reported using these agents *in vitro*.[20, 31, 54, 55] However, the ^{1}H background signal from surrounding tissue can complicate the interpretation of observed contrast in the images, as hypointensities can also be caused by other sources like blood clots, cavities and/or bleedings.[10, 15, 22] Moreover, the quantification of the number of cells is not possible *in vivo* using this approach.

4.2.2 Lanthanide chelates and Manganese based agents

Paramagnetic agents like lanthanide chelates and manganese-based agents are commonly used for their influence on the T_1 relaxation time. In order to influence the T_1 relaxation time, the paramagnetic agents have to be in close proximity of the protons in the water molecules,[20, 56] resulting in a lower

sensitivity for this technique compared to T_2 influencing agents. The advantage of these agents is that they provide bright spots in the MR image (hyperintensities) and therefore blood vessels, air cavities and hemorrhages are less likely to be confused for the paramagnetic agent.[20, 21]
Manganese-based agents like $MnCl_2$ and MnO_2 have also been tested for the use as contrast agents. Unfortunately these salts are too toxic to be used in a clinical setting.[20]

The detection of paramagnetic agents is generally difficult because they only induce subtle changes in the images compared to the background ^1H MRI.[14] Another disadvantage is that the mechanism of paramagnetic agents, like Gd^{3+}, is strongly dependent on the interaction with H_2O molecules. When incorporated into cell compartments the contrast-enhancement can be quenched due to a lack of water exchange through the membrane.[57]

Totally different types of contrast agents are compounds containing ^{19}F-nuclei.

4.2.3 Heteronucleair MRI: ^{19}F containing compounds

The first suggestion for the use of ^{19}F tracer compounds in MRI was made by Holland *et al.* only a few years after the development of ^1H MRI.[13, 58] ^{19}F is a very promising nucleus for the use in MRI because the natural abundance of the MR active ^{19}F is 100%. The resonance frequency of fluorine only slightly differs from hydrogen, making it possible to conduct ^{19}F MRI on ^1H MRI hardware by using optimized coils for dual $^1H/^{19}F$ imaging.[11, 26, 35] Fluorine has seven electrons in its valence shell compared to only one for hydrogen. Therefore the influence from the environment on the fluorine chemical shifts is larger than for hydrogen.[26] Biological tissue contains only a low natural concentration of fluorine of about 0.0066 mol/L[51] resulting in no signal from background tissue.[9, 11] The only fluorine found in the human body are solids in bones and teeth, which have a very short T_2 relaxation time and are therefore difficult to detect with ^{19}F MRI.[22, 30, 58]
The ^{19}F signal provides an unique label for tracking cells.[22] Different types of cells can be labeled *ex vivo* before injection. The cells can be placed in their anatomical context by overlaying the ^{19}F image with a regular ^1H image.[10, 11, 14, 22, 36] In addition, perfluorocarbons have been used, tested and evaluated extensively over the past 20 years so already a lot is known on their bioactivity, toxicity and degradation, as was already discussed in chapter 3.

The gyromagnetic ratio of the ^{19}F nucleus is comparable to that of ^1H, resulting in a similar sensitivity of ^{19}F MRI compared to ^1H MRI.[14, 22, 24, 26, 51] There is a linear relationship between the amount of ^{19}F spins and the intensity of the signal.[10, 16] Consequently, the signal intensity in ^{19}F MR images can be directly related to a useful quantity index by comparing the signal intensity to that of a reference sample like trifluoro acetic acid (TFA).[10, 11, 14, 22, 30, 36] This allows determination of PFC cell loading and quantification of the amount of cells *in vivo* once the cell loading is known.[18, 35] Each PFC has its own specific resonance frequency making it possible to distinguish between different cells labeled with different

agents *in vivo* at the same time.[16, 26, 27, 59] In such experiments, the signal intensity is directly related to the concentration of one type of PFC. For imaging of one specific PFC the resonance frequency of that specific PFC should be set as the frequency of the RF excitation pulses.[27]

The tracking of cells labeled with ^{19}F containing contrast agents is fundamentally different from the use of paramagnetically labeled cells.[22, 58] Paramagnetic agents influence the T_1, T_2 and/or T_2* values of the surrounding protons in water molecules and create hypointense or hyperintense spots in $T_2^{(*)}$- and T_1-weighted MRIs respectively.[6, 10, 15, 20, 22, 56] In contrast, the ^{19}F nuclei acts as a tracer, which is directly detected in the labeled cells because it has its own, intrinsic, signal.[6, 11, 58]

5. PFC nanoemulsions

5.1 Chemical structures

Perfluorocarbons have been studied for many years. They are one of the most stable chemical compounds and show exceptional chemical and biological inerness.[1, 2, 4-8] The chemical structure of a particular PFC is important for its use in MRI. An ideal PFC for MRI should contain many chemically equivalent fluorine atoms to minimize the amount of resonance frequencies measured in order to maximize the sensitivity and prevent chemical shift artifacts.[6] Chemical shift artifacts are causes by structures giving more than one resonance frequency, this will result in a shift in the position of the image. (figure 4) Therefore in particular symmetric, linear and macrocyclic PFCs are attractive for the use in ^{19}F MRI.[23] An overview of the structures of several PFCs is provided in Figure 5

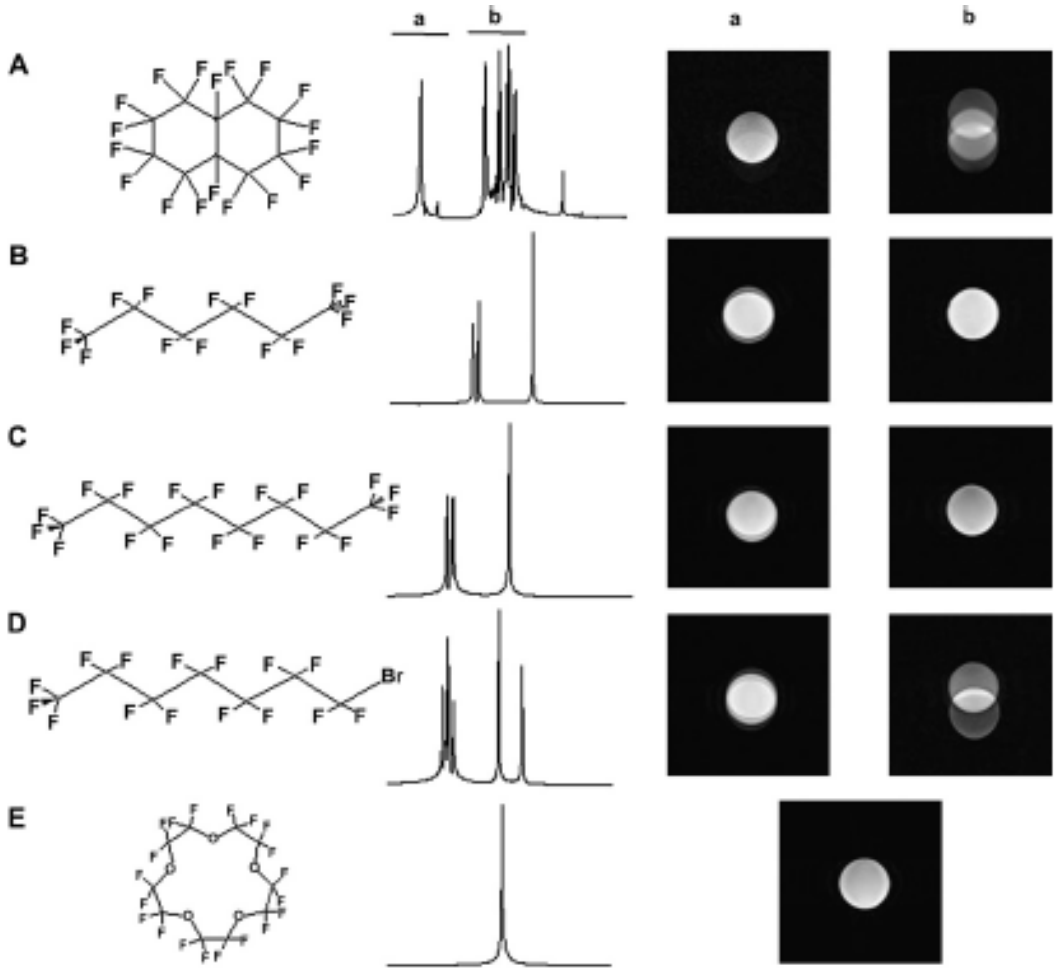

Figure 4: The structures of several PFCs and their ^{19}F NMR spectrum. In the NMR spectrum the resonance frequencies are indicated that are used for MRI, a. and b. correspond to the images obtained. Structure A: perfluorodecalin; B: perfluorohexane; C: perfluorononane; D: perfluorooctylbromide (PFOB); E: perfluoro-15-crown-5-ether (PCE). Figure taken from Srinivas et al.[34]

Perfluorooctylbromide (PFOB) is the compound that has been most extensively studied.[6, 27, 50, 59] Compared to most other PFCs, PFOB is slightly more lipophobic due to the bromine. However, the NMR spectrum of PFOB, with 8 peaks at different resonance frequencies, is quite complex, and is therefore not an ideal perfluorocarbon for imaging purposes.[6]

Perfluoro-15-crown-5-ether (PCE) is a macrocyclic structure, resulting in only one resonance frequency at -92.5ppm. All its 20 fluorine atoms are chemically equivalent. Another perfluoroether used for imaging purposes is perfluoropolyether (PFPE). PFPE is a linear polyether with many equivalent fluorine nuclei depending of the size of the polymer. The major resonance frequency of PCE is around -91.5ppm. Linear structures, such as PFPE, have the disadvantage over cyclic structures like PCE that their NMR spectrum is slightly more complex. However, if the linear chains are sufficiently long the resonance frequencys from the end groups are below the detection limit and exert almost no contribution to the detected signal in the ^{19}F MR images.[36]

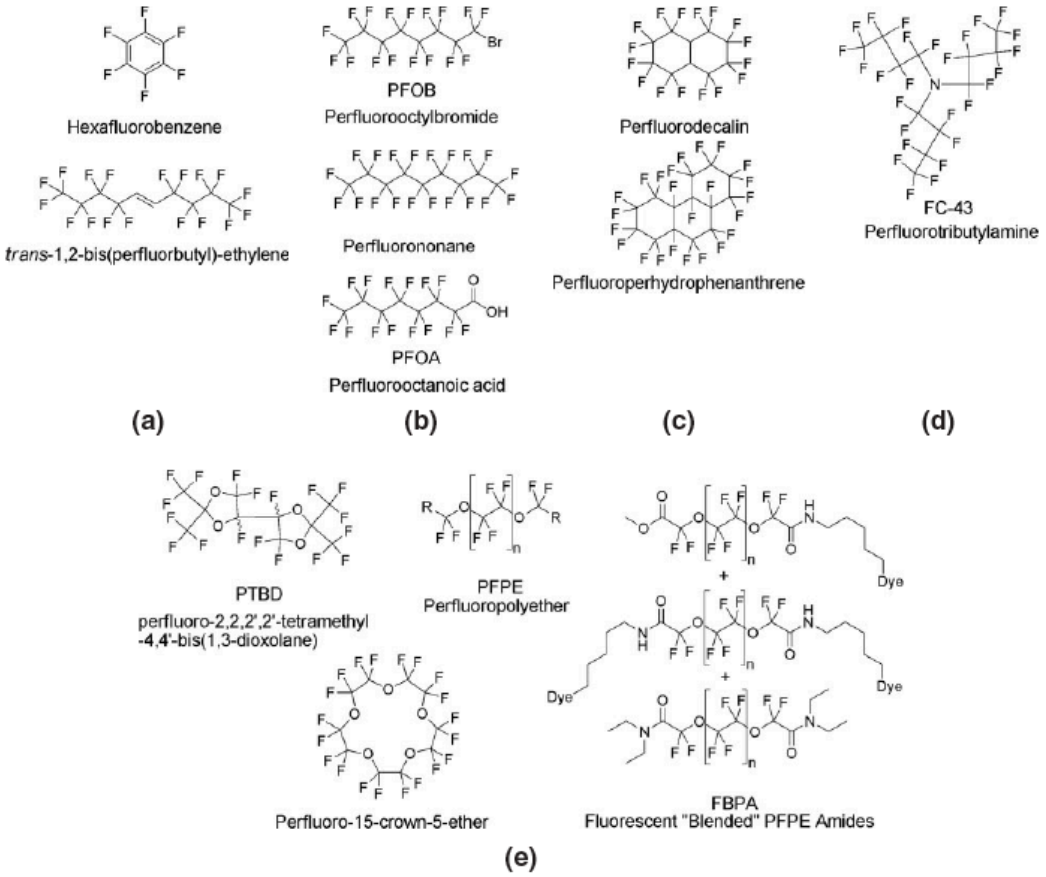

Figure 5: Structure from several PFCs. Only perfluoropolyether (PFPE), perfluoro-15-crown-5-ether (PCE), perfluorodecalin and perfluorooctylbromide (PFOB) have been used in MR imaging of cells. Figure taken from Janjic et al.[6]

The chemical shifts of the PFCs are not altered when incorporated in cells.[6, 14, 34, 38] The line shape of cells labeled with PFPE is a single narrow peak and is comparable to the signal of the pure compound.

5.2 Commercially available nanoemulsions

CS-1000 (Cell Sense) is a nanoemulsion produced by Celsense in Pittsburg, USA, which is patented as a MRI tracking product. It was developed to 'facilitate the internalization of the reagent *in situ* into cells without phagocytic ability'.[10, 30] The nanoemulsion is called CS-1000 and contains linear PFC polymers, with an average diameter of 170 nm at a concentration of 100mg fluorine per mL.[10]. The linear PFC polymers are optimized to have only one major resonance frequency. The actual chain length of the polymers is not revealed. Cells can be labeled effectively with CS-1000 without the need of a transfection agent.[10, 11] The FDA approved the start of a clinical trial for the use of CS-1000 in a human in May 2011. The recruitment of volunteers will commence in the beginning of 2012.[11] Also a dual mode nanoemulsion of Cellsense is commercially available as CS-DM Green. CS-DM Green is conjugated with a FITC fluoropore with emission and excitation wavelengths at 495 nm and 521 nm respectively.[11] This nanoemulsion was already used for the labeling and tracking of NSCs[15] and DCs.[10, 19]

Another product of Celsense is V-Sense.[17] V-Sense is a nanoemulsion with an average size of 145 nm, which contains 20% volume fraction of perfluorocarbon polymer in a buffered solution. Alternative formulations of V-Sense with different perfluorocarbons are also available, including emulsions with PCE (VS-580) and perfluorodecalin (VS-462).[17] V-Sence containing PCE has already been used *in vivo* for imaging inflammation after organ transplantation (see also chapter7.3.2.).[22]

Several other PFC nanoemulsions are commercially available including:

- Oxygent™, Alliance, Pharmaceutical Corp., contains F-octylbromide and F-decylbromide
- Optison®, Amersham health, Inc., contains perflutren (perfluoropropane)
- Sonovue®, Bracco Diagnostics, Inc., contains sulphurhexafluoride
- Imagent®, Alliance Phamaceutical Corp.

However, only Oxygent™ has been previously used in imaging experiments.

5.3 The preparation of nanoparticles

Alternative to commercially available nanoemulsions, the synthesis of perfluorocarbon nanoemulsions is also widely described in literature.[2, 7, 14, 16, 18, 23, 24, 27, 29, 32, 36, 48, 60-62] Three examples of the preparation of nanoemulsions are described in the upcoming paragraph:

1. PCE with Lissamine rhodamine B fluorescent label
2. PFPE amide with covalently bound fluorescent label (either BODIPy-TR, FITC or Alexa647)
3. PCE with rhodamine fluorescent label and a targeted ligand for molecular imaging

The one below is the preparation for perfluorocarbon nanoparticles containing PCE and a fluorescent label reported by Flögel and coworkers.[18] First, a solution

of egg lecithin in an isotonic phosphate buffer (10 mM phosphate, 150 mM HCl, pH=7.4) was stirred for 30 minutes at room temperature. Then the fluorescent label Lissamine Rhodamine B was added. The resulting mixture was dissolved in ethanol after which the solvent was removed under reduced pressure and the residue was completely dried under high vacuum the yield a lipid film. The lipid film was gently hydrated with buffer solution before PCE was added. The suspension was first treated with a high performance dispenser at 14000 rpm for 2 minutes and afterwards high pressure homogenized. In the last step the nanoemulsion was filtered through a 0.22µm filter. The nanoemulsion was stored at 6°C until used.[18]

Before usage the nanoemulsion was characterized. The size of the particles was determined to be 130 nm on average. After storage for 10 weeks at 6°C no changes in size or zeta potential were observed. For a more elaborate description of the procedures used by Flögel and coworkers see the data supplement.[18]

A self-delivering dual mode fluorescent blended PFPE amide has been developed by Janjic and coworkers.[23] They achieved to label fetal skin derived DCs and primary T-cells *ex vivo* with a cell loading of 10^{11}-10^{13} spins per cell within 3 hours. The nanoemulsion was prepared with a 9:1 v/v ratio of PFPE oxide and (fluorescent) PFPA added together while continuously vortexing. Next, aqueous solutions of F68 and PEI were added and microfluidized. All the structures of the components of this nanoemulsion are shown in figure 6. The resulting nanoemulsions were filter-sterilized and stored at 4°C until usage.

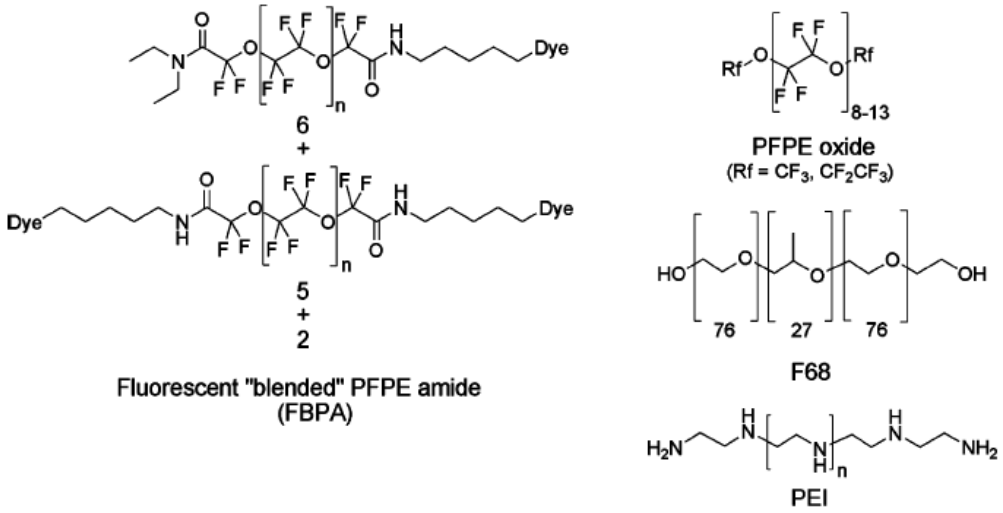

Figure 6: Chemical structures of all the components in the dual mode fluorescent PFPE amide namoemulsion. Figure taken from Janjic et al.[23]

A non-fluorescent nanoemulsion was prepared in the same manner; only instead of the fluorescent dyes a diethylamide was coupled at the ends of the PFC to deactivate the free amides.[23] For the fluorescent nanoemulsions three different dyes; BODIPy-TR, FITC and Alexa647. The nanoemulsions were characterized with ^{19}F NMR and dynamic light scattering. The average size of the emulsion was 160-190nm. Shelf and serum stability was tested and nanoemulsions with

Alexa647 as dye showed an increase of particle size by 30% after 3h in serum, possibly caused by the anions of Alexa647. The nanoemulsions with other dyes were found to be stable.

For *in vivo* experiments it is sometimes difficult to obtain high enough quantities of ^{19}F at the desired places. Therefore targeted nanoparticles were developed. Targeted particles contain a specific ligand that binds to a biomarker. More on this topic can be found in chapter 7.3.
A method for the preparation of targeted nanoparticles was developed by Winter *et al.*[63] The emulsion contained 20% (v/v) PCE, 1.7% (w/v) glycine in deionized water and 0.135 mol% rhodamine. To enable attachment of a special targeting peptide 0.09 mol% of MPB-PEG-DSPE-peptide was added to the surfactant commixture and the lipid film was reacted with a VCAM-1 targeting peptide in a 1:1 ratio. The MPB-PEG-DSPE-peptide contains a maleimide group that reacts with the side chain of cysteine forming a thioether bond. The mechanism of this reaction is shown in figure 7.

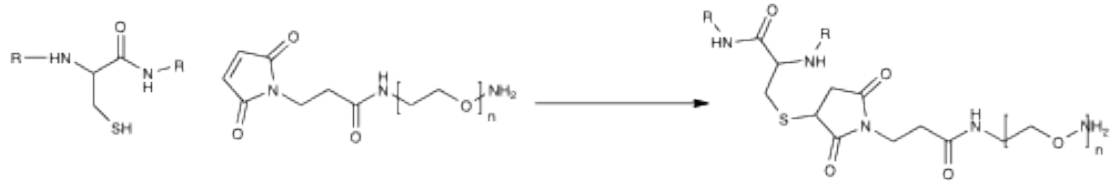

Figure 7: Mechanism of the reaction between maleimide and the side chain of cysteine forming a thioether bond. The reaction occurs spontaneously upon mixing the two reagents together.

Everything was added together, sonicated and emulsified at 20 000 PSI for 4 min. in an ice bath. The efficiency of the conjugation of the peptide to the nanoparticles was analyzed with a BCA protein assay in the supernatant after centrifuging. The conjugation efficiency was calculated to be 87.9% ± 0.075.[32, 63]

5.4 Degradation of nanoemulsions

PFC nanoemulsions can be formulated as kinetically stable emulsions. The droplet size of the emulsions varies between 20nm and 500nm in diameter.[6] Oswald ripening is the most common degradation mechanism for nanoemulsions.[4, 6, 64-66] The driving force in Oswald ripening is the chemical potential inside the droplets. Single molecules diffuse from the smaller droplets to the larger droplets where the chemical potential is smaller.[4, 66] Due to Oswald ripening particles will gradually grow, which is the major problem for the formulation of stable nanoemulsion.[6] The choice of emulsifier technique, surfactant, the molecular shape and weight of a PFC molecule can greatly influence the rate of Oswald ripening .[4, 6, 64-66] For instance, Oxygent™ consists of mainly PFOB with the addition of a small percentage of perfluorodecylbromide and therewith reducing the rate of growth.[4] But the principle of Oswald ripening in nanoemulsions is not only dependent on the chemical potential of the droplets. The diffusion coefficient and the solubility of the perfluorocarbon as well play an important role,[64] as well as the structure of the PFCs themselves.[66]

Nanoemulsions of long, branched perfluorocarbons are more stable than emulsions of smaller PFCs.[66] In some cases degradation proceeds faster than others. An example hereof is the Alexa647 labeled PFPE amide, as also mentioned in the previous paragraph. The nanoemulsions with BODIPy-TR and FITC labels were found to be stable, while the nanoemulsion with Alexa647 only had a lifetime of 3 hours.[23]

6. Cell labeling and detection limits

6.1 Cell labeling

A typical cell labeling setup is incubation with the nanoemulsion for 3 hours or more.[11, 23] A sufficient cell loading can be obtained in DCs, NSCs/NPCs and T-cells without the use of an transfection agent, which is an advantage for the use of PFC in cell labeling experiments since most transfection agents are not approved for clinical use.[35] However, in some types of cells the use of a transfection agent increases PFC loading levels. For example; cationic particles are taken up more effectively by mouse NSCs[29] and the use of the cationic transfection agent lipofectamine in a PFPE emulsion strongly enhances the uptake by DC cells (~26 fold).[14] A method for coating PFPE nanoparticles with cationic ligands was already developed and evaluated.[14, 29, 36] However, the use of transfection agents might enhance toxicity to the cell lines and manipulate the cell culture.[19, 27]
Alternatively, several types of cells have also been labeled without the use of any additives,[19] for example the uptake of a labels containing PFOB or PCE were taken up by NSCs without any problems.[27] In this case, loading levels are typically higher in phagocytic cells, like DCs, than non-phagocytic cells, such as T-cells and NSCs.[23, 35] An overview of the cells used in experiments described in this thesis is provided in box 1.

Box 1: Overview of the cells used in experiments described in this thesis

Dendritic cells (DCs) are antigen-presenting cells that posses the ability to stimulate and regulate responses of several types of T-cells. A lot of research is done on their potential role in the treatment of immuno disorders,[14] cancer and infectious diseases.[19]

Neural stem cells (NSCs)/neural progenitor cells (NPCs) are self-renewing cells that have not differentiated yet. Stem cells can differentiate into a variety of different cell types. Neural stem cells obtain the ability to differentiate into neurons and therefore they widely tested in regenerative therapy in neurodegenerative diseases.

T- cells or T-lymphocytes play a role in the cell-mediated immunity and are known to accumulate at sites of inflammation.

^{19}F tracking of cells has the same limitations as with the use of other (paramagnetic) cell-labeling agents. The tracking of cells is limited by the cell division rate and the life time of cells.[58] As a function of time the number of ^{19}F nuclei per cell will decrease due to cell division, which contributes to the difficulties encountered in quantifying the amount of cells[30, 36] and discrimination between living and death cells.[58] *In vivo* administration only allows labeling of RES cells while *ex vivo* labeling allows the use of different, and more specific, types of cells. Cell loading (^{19}F nuclei/cell) can be determined with the aid of a reference sample.[10, 14, 19, 23]

In vivo determination of the intracellular retention time of labeled DCs showed that the ^{19}F signal decreased to 15% of its initial value due to cell division within 5 days.[14] In case the cell division rate is known[30], quantification of the number

of quickly dividing cells is possible by correcting the error in the estimation.[30, 37] However, exocytosis of the PFCs or cell death followed by the transfer of the labels to phagocytes can also contribute to an underestimation of cell numbers.[10, 19, 36]

Immunohistochemistry on tissue and the usage of a dual mode reagent containing a fluorescent dye can give more information on cell identity (e.g. if the labels are transferred). Therefore, in cell tracking studies often a second, fluorescent, component is employed for validation of the MRI data. Fluorescent dyes often are incorporated into the nanoemulsions by mixing them with the PFC in the preparation of the nanoemulsions. Recently, Ahrens *et al*. have reported the development of a new type of PFC.[23] These dual mode reagents, also shown in figure 5E, are made up from a linear PFPE that is covalently bound to a fluorescent dye.[23]

In most situations a large part of the cells labeled with nanoparticles remain in the circulation where their concentration is too low to be detected *in vivo*.[18, 36] In cases when the concentration of circulating nanoparticles is high enough to be detected, the background signal caused by those particles can be canceled out using a rapid acquisition with refocused echo's (RARE) sequence while acquiring the ^{19}F MRI.[18] A RARE sequence is a type of fast spin echo (FSE). It measures the electromagnetic emission of nuclei (echo) at different time points. Because multiple echoes are acquired during the imaging time the echoes of moving particles are canceled out.[51, 67]

6.2 In vivo selectivity for monocytes/macrophages

When injecting PFC nanoemulsions *in vivo* into a test subject cells of the RES will take up the nanoparticles selectively. Some examples for the selectivity of PFCs are provided by Smith and Flögel and coworkers.[18, 48]

Smith and coworkers reported measuring the uptake of Oxygent™ emulsions by a differentiated human monocyte cell line (THP-1). The THP-1 cell line was differentiated by treatment with PMA (Phorbol-12-myristate-13-acetate) into macrophage like cells. A control cell line was treated with Cytochalasin-B to limit their phagocytic ability. Both cell-lines were incubated with a fluorescence-labeled Oxygent™ emulsion. The fluorescence of the cells was measured at several time points. It was found that the macrophage-like cells take up a significant higher amount of the Oxygent™ emulsion than the control.[48]

The uptake of a PCE emulsion into monocytes/macrophages was also investigated by Flögel and coworkers in a group of 30 mice. At day 0 each mouse received the PFC emulsion via the tail vein. At days 1-7 blood analysis was performed on 3 mice at every time point. A ^{1}H/^{19}F MRI was performed *ex vivo* as well as flow cytometry and blood count experiments. The ^{1}H/^{19}F MR Images are shown in figure 8. Observed was that the PFC emulsion mainly accumulates in the mononuclear cells when administrating the emulsion *in vivo*.

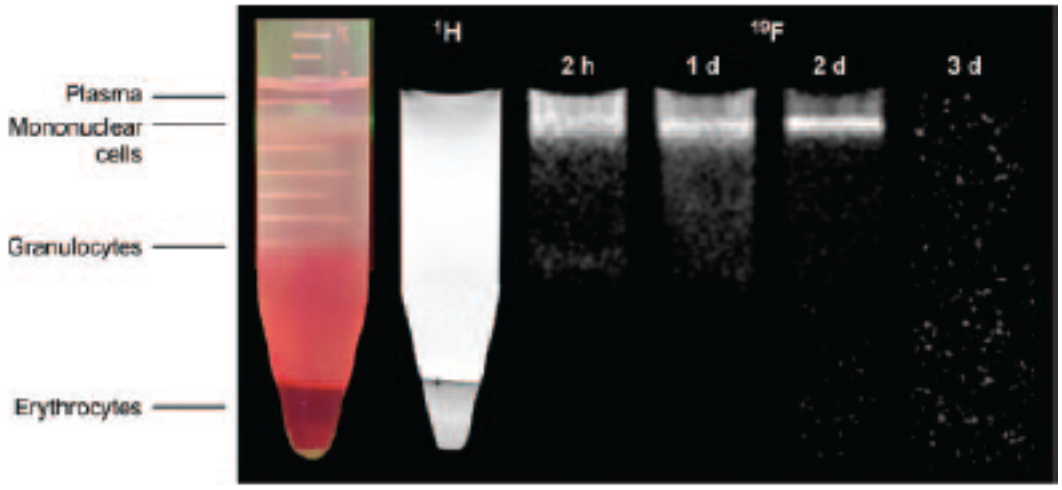

Figure 8: Uptake of PFC emulsion at different time points
The illustration shows the ^{1}H image and ^{19}F images of a blood sample after density gradient centrifugation. A time dependent uptake of the PFCs in the mononuclear cells is seen. At day 3 the PFCs were cleared from the bloodstream. Illustration taken from Flögel *et al.*[18]

6.3 Effect of labeling on the viability and proliferation of cells

When labeling cells with contrast agents their function phenotype and proliferation should not be altered. Therefore, they should be validated with specific assays and histology tests *ex vivo*, like for example a tryphan blue exclusion method, which measures necrotic cells,[23, 27] 10 nonyl acridine orange (NAO) assays, which measure mitochondrial lipid cardiolipin that is associated with early stage apoptosis and/or MTT assays, which measures mitochondrial activity. Alternatively, in certain cells, such as DCs, the interleukin production and T-cell stimulation of the cells is tested to asses cell function. Moreover, immunostaining and FACS analyses[23] can be done to measure antigen expression on cell surfaces.[19]
Several types of cells have already been labeled with PFCs, including dendritic cells (DC), T-cells and neural (stem) cells. Safe loading levels of PFCs are found to be in the range of 10^{11} – 10^{13} fluorine atoms per cell without any signs of toxicity.[6, 23, 36, 37]

Dendritic cells
Labeling DCs with the commercially available nanoemulsion CS-1000 lowers the cell viability to 80% compared to the control, as demonstrated by Bonetto et al.[10] The cells have been shown to internalize the label effectively without the addition of detergents with a loading of 1.7±0.1 x 10^{13} ^{19}F atoms per cell.[10] Comparison with the control cell line does not show differences except for size. The labeled cells show no change in expression of maturation factors and in expression of proteins after mRNA electroporation and no difference in T-cell activation was found when mixing the labeled DCs with lymphocytes in different ratios.[10] Also, labeling DCs with PFPE nanoemulsions showed that the labeling had minimum adverse effects on the proliferation, metabolism, phenotype and toxicity.[14, 19]

T-cells

Labeling of leukemic T-cells and adherent- and phagocytic DCs with FBPA appeared not to have any influence on the proliferation and morphology of the cells even at the highest doses. However, the viability of the labeled cells was significantly lower, i.e. 70% compared to the untreated cells.

Ahrens *et al.* labelled T-cells with PFPE nanoemulsions. They observed a slight decrease in CD4 receptors on the T-cells when using a transfection agent (lipofectamine) for cell labeling.[36] The decrease in CD4 receptors did not seem to affect the function of the T-cells *in vivo.*[36] In a control experiment electroporation was used for cell labeling. The same cell loading was found and no decrease in CD4 receptors was observed. In contrast, the use of the transfection agent did allow significantly enhanced, i.e. 26-fold, uptake of the label by DC cells.[14]

6.4 Detection threshold

Certain challenges still persist in ^{19}F MRI concerning low concentrations of ^{19}F. A high enough concentration sometimes is hard to obtain when labeling cells *in vivo* with a passively accumulating contrast agent. Therefore in a lot of studies cells are labeled *ex vivo* followed by injection into the target. To circumvent this problem, targeted nanoparticles might be a solution because they specifically target cells by using a biomarker. A summary of the studies using molecular imaging is given in chapter 7.3. Another possibility is signal enhancement by incorporation of Gd^{3+} ions.[62, 68] Incorporation of Gd^{3+} can enhance the signal intensity up to 125%.[62] But there are also several examples in literature on labeling and imaging cells *in vivo* at sites of inflammation without the use of a specifically targeting ligand or the addition of Gd^{3+}. (Chapter 7.3)

The low concentration of ^{19}F compared to mobile water results in a significantly lower signal-to-noise ratio (SNR) of ^{19}F images than for ^{1}H images. However, due to the absence of ^{19}F background SNR of <5 is considered sufficient to distinguish cells from the background, even at clinical field strengths.[6, 10, 22, 24, 27]

The sensitivity of the ^{19}F nucleus is in the same range as ^{1}H, therefore detection limits are in the same order as ^{1}H MRI.[14] The detection limits for ^{19}F MRI are in the range of 10^{18} spins per voxel at a 1.5T clinical setting,[14, 59] For high field measurements the detection limit can even be lower. Bonetto *et al.* reported a detection limit of 10^{16} spins per voxel at 7T field strength,[10] which is also consistent with earlier reports on the labeling and imaging of murine cells with different agents at high field strength.[10, 23, 36] Flögel et al. reported a detection limit of 10^{6} monocytes/macrophages with a voxel size of 0.44µL after labeling *in vivo* at 9.4T.[18] In general the loading of cells *ex vivo* is around 10^{13} spins per cell in different cells resulting in a detection limit of 10^{3}-10^{4} cells for a high field measurement and 10^{4}-10^{5} cells in a clinical setting.[10, 11, 14, 27, 29, 36]

6.5 Signal enhancement by the incorporation of Gd^{3+}

With labeling and imaging of cells *in vivo* difficulties can be encountered because of low concentrations of ^{19}F spins. Neubauer and coworkers report enhancement of the ^{19}F signal by the incorporation in Gd^{3+} ions into the PFC nanoparticles due to local changes in the magnetic field induced by Gd^{3+}.[62] The Gd^{3+} particles should be in close proximity to the ^{19}F nuclei to have any interaction, asdemonstrated by studies showing that mixing Gd^{3+} with aqueous PFCs has no influence on the signal intensity.[62, 69] In contrast, the incorporation of Gd^{3+} into emulsions can give an increase in magnetic relaxation rate resulting in a signal intensity increase of 125%, allowing shorter imaging times with a similar resolution as imaging of PFCs without the incorporation on Gd^{3+}.[62] This is also shown in figures 9 and 10.

Alternatively, Gd^{3+} PFC nanoparticles have been extensively used in order to enhance the contrast in ^{1}H images.[70] This contributes to a new imaging strategy, in which particles can first be visualized in low spatial resolution ^{1}H images due to the Gd^{3+} induced hyperintense spots. Next, more localized ^{19}F images can be made.[59] Because PFCs are highly stable, these particles have a long circulation time *in vivo* as well, enabling to track and monitor cells over a period of several days to weeks.[71] The other advantage is the possibility to combine ^{1}H and ^{19}F molecular imaging with the use of one single particle.[26, 62]

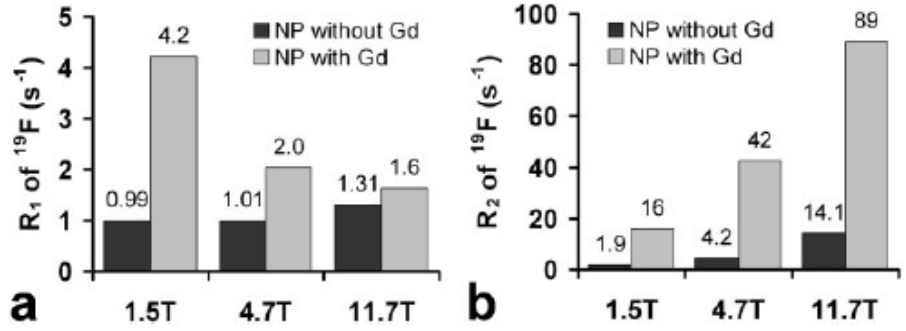

Figure 9: The graphs display the R_1 and R_2 ^{19}F relaxation at 1.5T. R_1 and R_2 represent the reciprocal values of the T_1 and T_2 relaxation times, respectively. The Gd^{3+} particles have to be in close proximity to the fluorine nuclei to influence their relaxation. Nanoparticles in an aqueous solution of Gd^{3+} chelates have no influence on R_1 relaxation rates and only slightly on R_2 relaxation rates. Incorporation of Gd^{3+} on the surface of the PFC nanoparticles has a large influence on the R_1 as well as the R_2 relaxation rate. The concentration of Gd^{3+} is given in mM. Figure taken from Neubauer et al.[62].

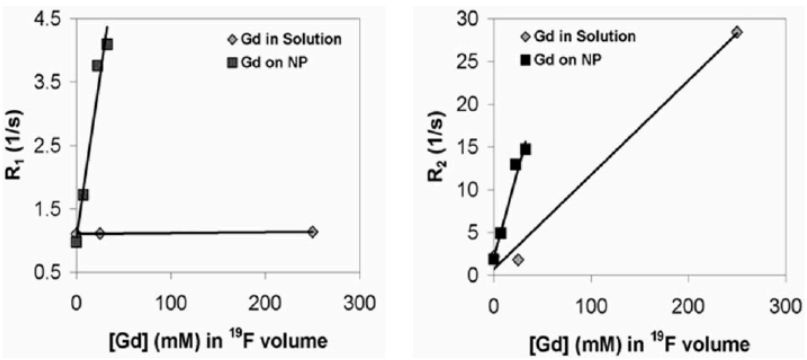

Figure 10: Bar-chart comparing R_1 and R_2 ^{19}F relaxation rates of PFC nanoparticles with and without a 30 mole% Gd^{3+}. Both R_1 and R_2 relaxation rates for the particles with incorporated Gd^{3+} are influenced and dependent on the field strength. Figure taken from Neubauer et al [62].

6.6 Location of the particles in the cells

The location of the PFC particles in labeled cells can be visualized with electron microscopy. Alternatively an additional tracer agent, like a fluorescent label, can be incorporated into the nanoemulsion. Figure 11 shows the images of DCs labeled with fluorescent PFPE nanoemulsions.[14] Fluorescence microscopy images (Figure 11A) showed that these nanoparticles are found inside the cells. Interestingly, these particles could even be observed with light microscopy (Figure 11B).

Similar results were described by Janjic *et al.*[23] for a nanoemulsion consisting of PBPA. Analysis with confocal microscopy showed vesicle-like structures of nanoemulsions in the cytoplasm of the T-cells. There were no indications of incorporation of the PFCs into cell membranes,[23] which was also not expected because of their lipophobic character.[11, 14, 19]

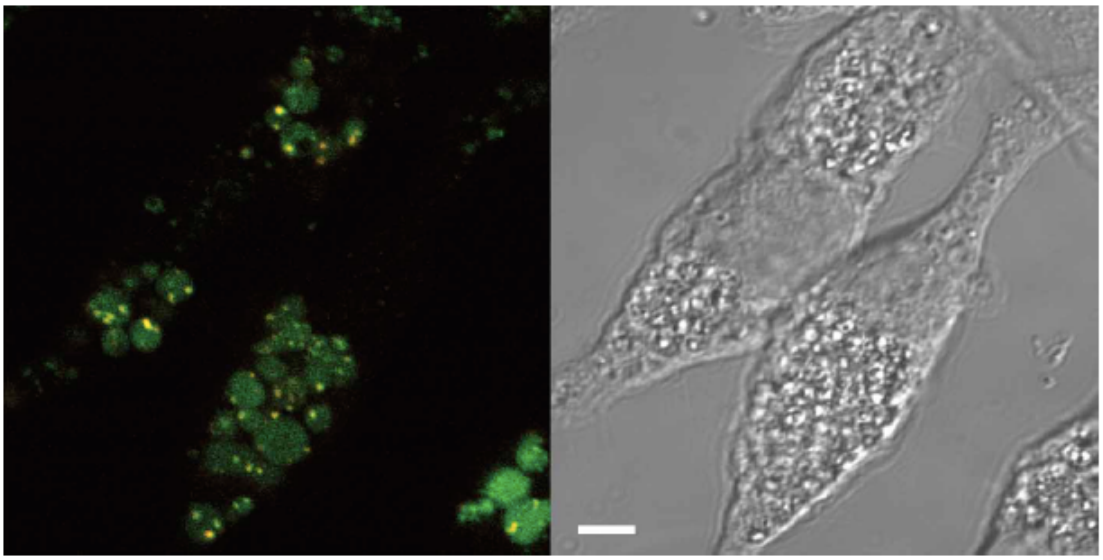

A **B**

Figure 11: Two images of PFCE labeled DCs. The nanoparticles are located inside of the DCs. (A) Confocal fluorescence microscopy imageof FITC-labeled nanoparticles. (B) differential interference contrast (DIC) microscopy image. Figure taken from Ahrens et al.[14]

7. Imaging experiments

Different types of MRI experiments are already reported in literature. ^{19}F MRI images should always be combined with a ^{1}H MRI for anatomical information. Different types of experiments are used, spin density weighted ^{19}F MRI provides mainly information on the area's where the concentration of accumulated PFC is the highest. Spin-echo-sequence and diffusion weighted MRI only show 'bound' or 'non moving' PFCs and enables to image only the accumulated PFCs without the noise of PFCs in the circulation.

A number of experiments have already been reported in the past years. The upcoming chapter will give a brief overview of all the experiments; *ex vivo* and *in vivo*, the outline of the experiment, the types of cells they use and their findings. In chapter 7.3 an overview will be provided on the use of molecular imaging with ^{19}F MRI.

7.1 *Ex vivo* cell labeling experiments

The most extensively used approach in perfluorocarbon research is the labeling of cells *ex vivo* before injecting them for *in vivo* imaging. *Ex vivo* labeling allows labeling of different types of cells, while *in vivo* administration of a nanoemulsion will only label RES cells. The advantages of this method are that *ex vivo* labeling of cells yields a most equal distribution in cell labeling[35] and it allows tracking of specific cells with the phenotype of interest.[6] After labeling *ex vivo* the PFC loading of the cells can be determined allowing quantification of the amount of cells *in vivo* after injection.

Dendritic cells

The principle of labeling and tracking cells with fluorine agents was proven by Ahrens and coworkers when they labeled dendritic mouse cells in 2005. They incubated fetal-skin derived- (FSDCs) and bone marrow derived DCs (BMDCs) for 18h with PFPE nanoparticles with a particle size between 100-200nm. Herewith they successfully showed that it is possible to track PFPE labeled DCs in a mouse model. Accumulation of the particles was observed in the lymph nodes close to the injection sites and later mainly in the liver, spleen and the lungs. *In vitro* assays on cell toxicity, proliferation, metabolism and phenotype showed that labeling the DCs with PFPE had a minor to no influence.[14]

Bonetto and coworkers published a study where human monocyte derived DCs were labeled with a commercially available PFPE nanoemulsion (CS-1000). A cell loading level of 1.7×10^{13} spins per cell was obtained with an acceptable viability of 80±6%. They showed that it is possible to do qualification of the number of cells. They compared their results with the use of a Gd^{3+} contrast agents and found a similar sensitivity. Their results show that ^{19}F MRI for quantitative cell detection and tracking can potentially be used in a clinical setting.[10]

Stem cells

Ruiz-Cabello *et al.* optimized the labeling of NSCs on culture plates with different surface charges.[29] They found out that cationic PCE nanoparticles are taken up the easiest by mouse NSCs. The labeled NSCs were transplanted into striatum of a mouse brain at two different doses. The signal stayed constant over 7 days and was visible until at least day 14. Immunohistochemistry on the mouse brain showed that after one week most of the cells were still present in the hemisphere and remained viable. Movement of the labeled cells after injection could be observed.[29] Similar results were obtained with labeling human NSCs with CS-1000 and placing them into mouse brains.[15]

Partlow *et al.* showed that it is possible to label and track stem/progenitor cells with different PFCs.[27] They showed that it is possible to distinguish between two types of PFC *in vivo* at experimental and clinical field strengths. *Ex vivo* labeling of the stem/progenitor cells was done by incubation for 12h with the PFC nanoparticles and yielded intracellular PFC concentrations up to 3pmol without the use of a transfection agent. Imaging times around 7 minutes provided a strong ^{19}F signal. Tuning to the desired PFC can be done by taking the most intense frequency of a specific PFC and tuning the RF output frequency accordingly. [27]

T-cells

The dual mode PBPA reagent developed by Janjic and coworkers was shown to be able to label T-cells in 3 hours by incubation *ex vivo*. Administration of the labeled cells to BALB/c mice showed accumulation of the cells in all major lymph nodes. The ^{19}F signal was proportional to the fluorescent signal measured at all concentrations of PBPA.[23]

Srinivas and coworkers tested the use of PFPE labeling and tracking of diabetogenic T-cells with MRI in the early stage of insulitis. In the development of diabetis T-cell migration in the pancreas is believed to be one of the first signs. In this study it was shown that the movement of T-cells towards the pancreas in a non-obese mouse model could monitored with ^{19}F MRI. The T-cells were taken from mice spleen and activated *in vitro*, labeled with PFPE and injected intraperitoneally. The control group was treated either with a cell free PFPE solution or labeled T-cells from BALB/c mice, which did not match the major histocompatability complex. It was found that the PFPE label is a good biomarker and a reliable estimation of cell numbers can be made.[36]

7.2 *In vivo* cell labeling experiments

In literature there is a lot of precedence for the uptake of the PFC particles by the RES.[2] The monocyte/macrophage system is able to take up PFCs very effectively and higher sensitivity is often obtained in experiments using RES cells compared to stem/progenitor cells.[18] Therefore these compounds are also found to be promising for *in vivo* labeling and imaging of monocytes/macrophages.[2] Below there are a few examples from literature that use PFCs to label inflammatory cells *in vivo*.

7.2.1 Tracking inflammatory cells after myocardial- and cerebrial ischemia

Flögel and coworkers reported labeling inflammation cells *in vivo* by systemically administration of a PCE emulsion. The preparation of the PFC emulsion used in this experiment is discussed in chapter 5. For the experiment mice models of myocardial infarction and cerebral ischemia were used. The PFC emulsion (average droplet size: 130 nm) was administrated via the tail vein.

Box 2: Myocardial infarction and cerebrial schemia
Myocardial infarction: Commonly known as a heart attack and is a result of the occlusion of coronary vessels. In the animal model used in this experiment the myocardial infarction was induced by creating an artificial blockade of the left anterior descending coronary artery. Cerebial ischemia: insufficient blood flow to the brain resulting in ischemic stroke. In the animal model used for this experiment cerebral ischemia was induced by photothrombosis (Rose Bengal).

A schematic overview of the amounts of test animals and the time schedule used in each experiment is shown in figure 12.

After surgery the animals were imaged accordingly. The cardiac ^{1}H analytical MRI was acquired using an ECG-respiratory-triggered fast gradient-echo cine sequence and ^{19}F images were recorded using multi-slice rapid acquisition with relaxation enhancement (RARE). For the cerebral ischemia studies ^{1}H and ^{19}F brain images were both acquired using multi-slice RARE sequences.

After PFC injection monocytes were effectively labeled, which made it possible to track the infiltration of the cells into the inflamed areas with an acceptable imaging time of about 20 minutes at 9.4 T. Rhodamine-labeled PFCs were used to investigate the nature of the labeled cells. The majority (≈80%) of the rhodamine positive cells were monocyte/macrophage cells (identified by the CD11b marker), a small amount of labeled cells were T-cells (<2%) and the rest of the rhodamine signal was originated from B-cells.

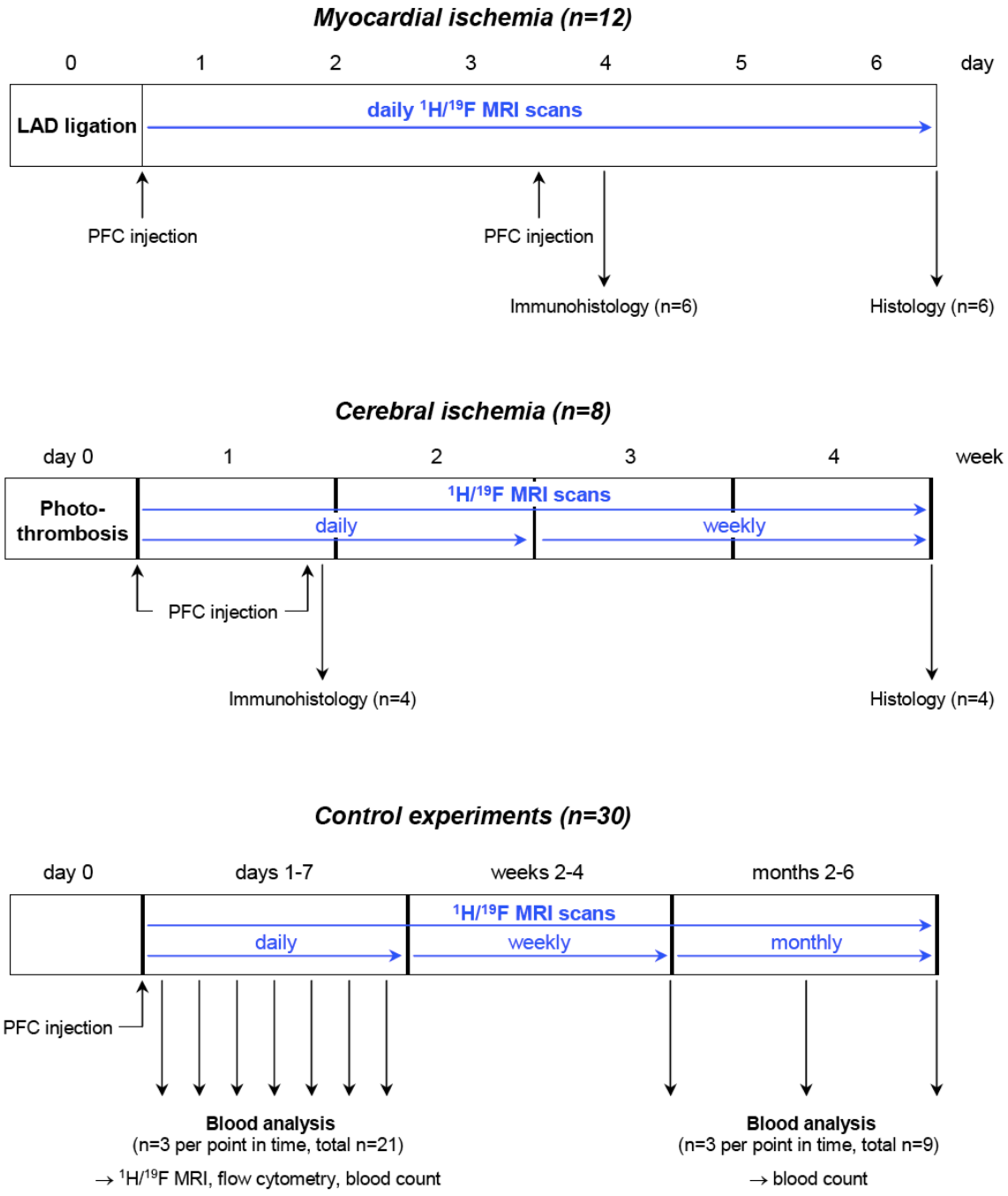

Figure 12: Overview of the time schedule and the quantities of rats per experiment. The chart gives the amount of animals used in either myocardial ischemia, cerebral ischemia and control experiments. It also shows at what time points MRI scans and other tests were done. Figure taken from Flögel et al.[18]

In the cerebral ischemia experiment infiltration of the PFCs into the infarcted region was observed starting at day 4 (no MRI image available). ^{19}F and ^{1}H images were acquired at day 7, 9, 12 and 19 after surgery. Over time movement of the PFC labeled cells was observed, matching the shrinking of the ischemia region. The $^{19}F/^{1}H$ images are shown in figure 13.

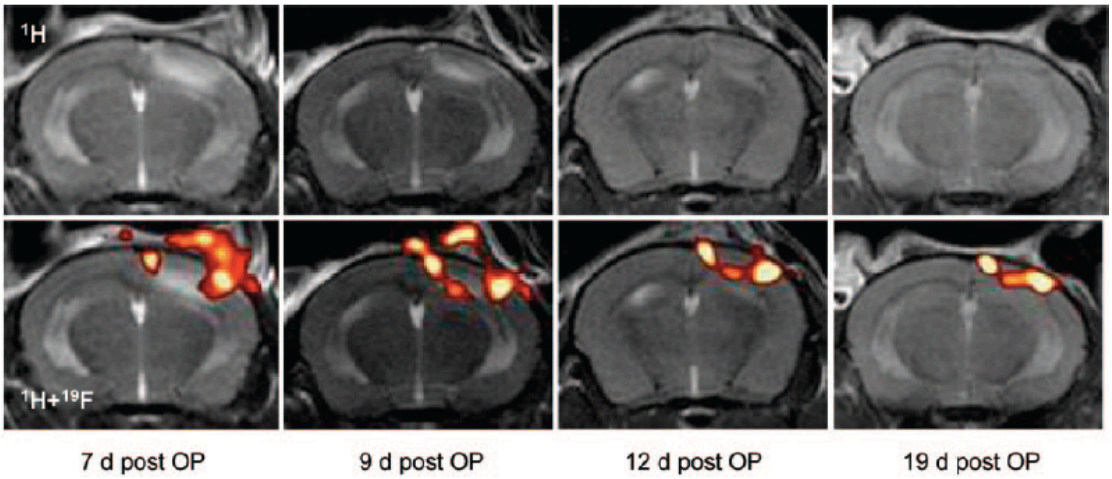

Figure 13: The localization of the labeled cells after cerebral ischemia
The top line of images is the ^{1}H image of a mice and the lower line of images is the ^{19}F and the ^{1}H image combined. The red highlighted signal is the ^{19}F image. The pictures were taken on day 7, 9, 12 and 19 after the surgery. The ^{19}F shows the rim of the ischemia area over time. Figure taken from Flögel et al.[18]

7.2.2 Tracking inflammatory cells after organ transplantation

Hitchens *et al.* reported an experiment in which they investigated the possibility of direct intravenous injection of a PFC emulsion and the possibility to track these particles *in vivo* to show accumulation of macrophages at organ rejection sites after transplantation.[22] Previous research conducted in the same group showed that macrophage accumulation is a suitable biomarker to monitor organ rejection. These studies involved the use of iron oxide particles to detect macrophage accumulation *in vivo*.[72]

Box 3: Organ transplantation
Organ transplantations can be allograft, isograft or xenograft of nature. Allograft is the most common type of transplantation when tissue or an organ is transplanted from a genetically not identical person. Isograft transplantation is less common, here the tissue or organ is coming from a genetically identical person (e.g. twin sister or brother). Xenograft transplantation is when the tissue or organ is transplanted from another, different organism.

A commercially available PCE nanoemulsions (V-sense (VS-580H), Celsense, Pittsburgh, USA) was used containing 30% w/v of the PFC with an average droplet size of 145 nm in diameter.[17] Rats underwent kidney (allograft) and heart (allograft and isograft) transplantations and were injected 24 hours after surgery with 1 mL (±3.6 mL/kg) of the PFC emulsion in the tail vein at a rate of 3 mL/h. An overview of the rats used in the experiment is given in table 2.

24 hours after administration of the PFC emulsion ^{1}H and ^{19}F images were acquired. ^{19}F images were made using a gradient recalled echo as a pilot scan and to identify PFCs in the circulation, followed by a spin-echo sequence to detect the labeled macrophages in the myocardium. A reference experiment was

performed with USPIO labeled macrophages. All animals were imaged *in vivo* 24 hours after administration and then sacrificed. Hearts and kidneys were also imaged *ex vivo* and the rejection rate of the organs was determined histopathologically. Fluorescent images were also obtained of the organs *ex vivo*.

Table 2: Overview of the rats used in the experiment

	Hearth	Liver	
Day 4		n=4 (allograft)	VS-580H
		n=1 (allograft)	Dextran-coated USPIO
Day 5	n=9 (allograft) n=3 (isograft)		VS-580H
	n=1 (allograft)		Dextran-coated USPIO
Day 26	n=1 (isograft)		VS-580H
	n=2 (allograft)		VS-580H with fluorescent label*
Control	n=3		VS-580H

*The fluorescent label dialkylcarbocyanine (4µL) was mixed with the VS-580 emulsion (1mL) just prior administration.

Blood clearance half time of the V-sense was determined in control rats. The rats were given an injection of 0.5 mL of the PFC emulsion. Blood was sampled over a period of 5 days. The concentration of the PFCs were measured using solution ^{19}F NMR (samples of 6µL-12µL) with TFA as a reference. The blood clearance half time was found to be 9.4 ± 2.6 hours.

7.3 Molecular Imaging experiments

For detection of a fluorine signal, a high concentration of accumulated nanoparticles is necessary to reach the detectable limit in a 1.5T clinical setting.[16] In most *in vivo* experiments high concentrations of accumulating PFCs are hard to obtain and therefore specific-targeted PFC nanoemulsions might be the solution.[16] Site targeted PFC nanoparticles are currently used in preclinical research and clinical trials are expected within years.[9]

7.3.1. Fibrin targeted PFC nanoparticles

Caruthers *et al.* reported an *in vitro* proof of principal that site-targeting nanoparticles can be applied in a clinical setting.[16] They showed that ^{19}F nuclei can be imaged using a 1.5T MRI in reasonable scan times. Two types of biotinylated nanoemulsions were synthesized containing two different PFCs; PCE and PFOB. The interactions of the nanoparticles with the fibrin cloths are achieved using a biotin-avidin interaction. The nanoparticles were also coated with a Gd-chelate to give them paramagnetic properties for contranst enhancement in a ^{1}H image. They showed that it is possible to measure, image and discriminate between both nanoparticles in various mixtures with steady

state echo techniques within 3 minutes of measuring time, as shown in figures 14 and 15 [16]

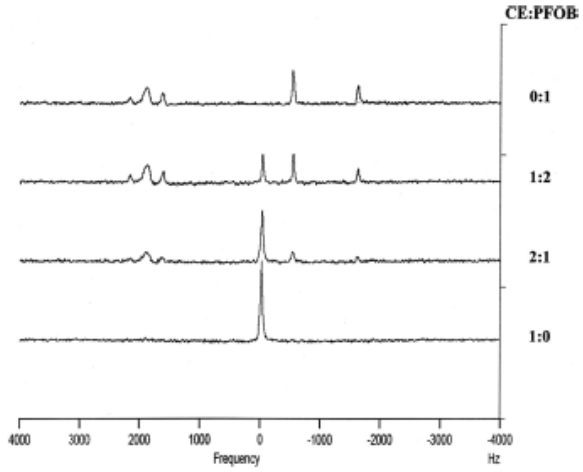

Figure 14 (above): The NMR spectra of PCE and PFOB nanoparticles in different mixtures. It is clearly seen that concentration can be determined from the intensity of the ^{19}F spectra and that the PFC chemical shifts do not alter. Figure taken from Caruthers *et al.*[16]

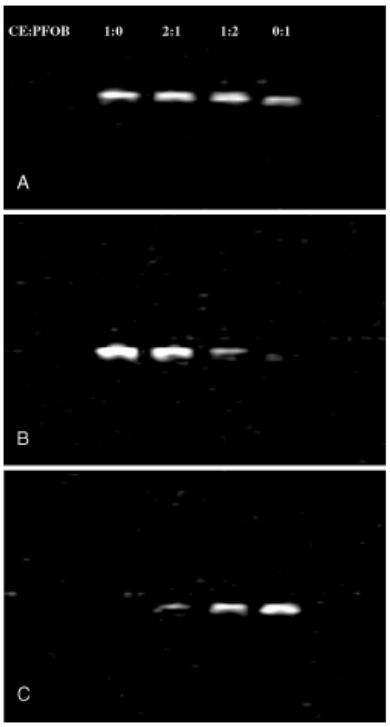

Figure 15 (right): ^{19}F Images of nanoparticles bound to fibrin cloths in different mixtures of PCE and PFOB. Images were obtained in 3 minutes. A. All fibrin cloths show brightness independent of the PFC mixture. B. Selective excitation on the resonance frequency of PCE gives only brightness in the PCE containing fibrin cloths. C. Selective excitation on the resonance frequency of PFOB only provides brightness in the PFOB containing fibrin cloths. Figure taken from Caruthers *et al.*[16]

7.3.2. α-β-integrin targeted PFC nanoparticles

Box 3: Aortic valve sclerosis
Aortic valve sclerosis is a cadiovascular disease that is most common among elderly people. A narrowed aortic valve causes the disease symptoms. Early detection and treatment can slow down the progression of the disease. In this study white rabbits, which have been fed a cholesterol diet, are used as a model.

The *in vivo* quantitative analysis of site targeted-nanoparticles can be difficult because of the background signal from unbound nanoparticles. Diffusion weighted ^{19}F MRI has been recently reported to circumvent this problem by selectively suppressing the ^{19}F signal from unbound nanoparticles.[9, 39]
Waters *et al*. showed the use of diffusion weighted MRI. A PFC emulsion containing PCE was used to image early development of aortic valve sclerosis. The emulsion was prepared with 0.093 mole% of vitronectin to give it its targeting properties.

Box 4: Vitronectin
Vitronectin is a glycoprotein involved in cell adhesion and is specifically bound by the $\alpha_v\beta_3$-integrin. In the mouse model used (K14-HPV16) the α_v-β_3-integrin is up regulated.

By using a diffusion gradient it is possible to distinguish between bound and unbound particles. Figure 17 shows the rapid decay of the signal of unbound particles in the control mice versus the persistent signal in the K14-HPV16 mice. This indicates that the nanoparticles specifically bind the up-regulated α_v-β_3-integrin present in the K14-HPV16 mice.[39]

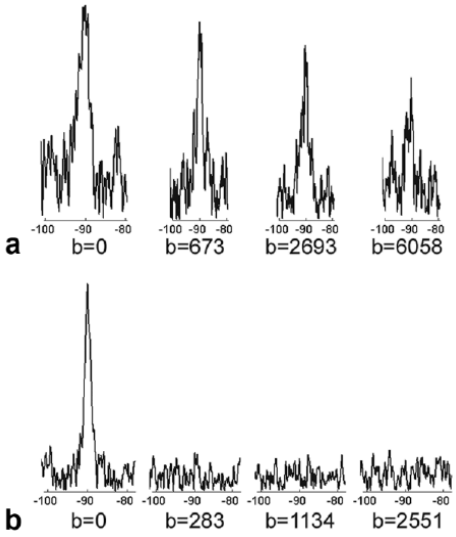

Figure 17 (left): Diffusion weighted ^{19}F spectra. X-axis values are given in ppm with trichlorofluoromethane as a reference. (a) Measured in K14-HPV16 mice. The spectra show persistent fluorine signal at large b-values. (b) Measured in the control group. Quick decay of fluorine signal is observed. Figure taken from Waters et al.[39]

Figure 18: The graphs show the decay of the fluorine signal as a function of the b-value. For the control (filled symbols) the decay is faster that for the K14-HPV16 mice (open symbols). Figure taken from Waters et al.[39]

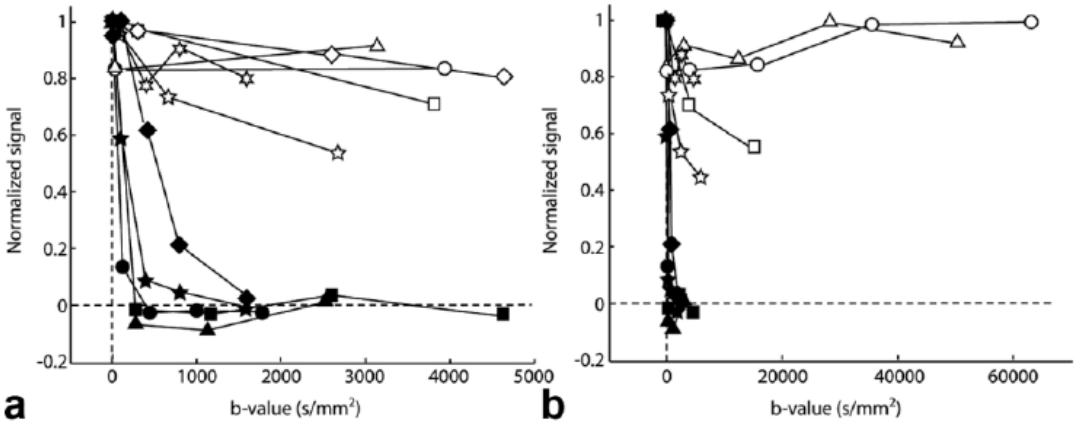

8. Conclusions and future directions for cellular ^{19}F MRI in brain disorders

Over the past years several studies have been published on the use of PFC nanoemulsions in MRI imaging on different cells and disorders.[3, 5, 6, 9, 10, 13-16, 18-20, 22-24, 26-29, 33-37, 40, 41, 49, 58-60, 62, 63, 70, 71] The labeling of cells with ^{19}F containing perfluorocarbon particles is a valuable strategy with several advantages compared to labeling strategies with paramagnetic agents; a technique that has been frequently employed for monitoring cells in the in the brain after brain injury.[18, 29, 41] For instance, the use of iron oxide particles for imaging of brain injuries where there is a possibility of hemorrhage can give a false positive.[10, 15, 22] For those cases, the use of perfluorocarbon particles for ^{19}F imaging would be good alternative.[29] Natural tissue does not contain any fluorine and therefore ^{19}F MRI is very selective for labeled cells. A SNR <5 is already sufficient to distinguish cells from the background. Because there is no intrinsic fluorine signal from the background a ^{1}H MRI is always needed for anatomical information. Perfluorocarbons, in contrast to paramagnetic agents, are not metabolized or degraded inside the body[18], instead they are excreted in a few days to weeks.[2, 42, 48] Additionally, there have not been any indications of toxicity to or major effect on the viability of cells even at very high PFC loading levels.[6, 23, 36, 37]

In vivo PFC nanoemulsion are specifically taken up by macrophages/monocytes, making it possible to track these cells while they move into inflamed areas in the body. Flögel and coworkers showed that it is possible to *in vivo* label and trace cells after artificially induced myocardial infarction and cerebial ischemia in mice.[18] They showed that at the regions of cerebrial- and myocardial ischemia monocytes, roughly 80% of the signal was originated from monocytes. The ^{19}F signal could be visualized up to 19 days and matched the schrinking of the ischemia region.[18] When labeling cells *ex vivo* it is possible to track DCs, NSCs/NPCs and T-cells as well. For example, intrastriatal-injected PCE-labeled NSCs can be visualized for up to 14 days inside of the brain of healthy mice.[29] This enables researchers to track the movement of specific cells and for example validate the efficacy in stem cell therapy in neurodegenerative diseases and the loss of functions after brain damage.[15]

The sensitivity of ^{19}F MRI is comparable to gadolinium-based agents, but less than for iron oxide particles, where single cells can be visualized *in vitro*.[55] For ^{19}F labeling of cells mostly a dual mode nanoemulsion is used, either containing a Gd^{3+} agent or a fluorescent probe. For imaging purposes the most common PFCs used are PCE, PFPE and PFOB, because they contain a large number of chemical equivalent fluorine nuclei that give a high sensitivity without inducing chemical shift artifacts.[9] Currently several commercially available nanoemulsions, containing PCE, PFPE or PFOB, which are optimized for ^{19}F MRI, are readily available.[11, 17] They have already been used for labeling DCs[10, 19], NSCs[15] and monocytes[22] *in vivo*.

Over the past years a lot of research has been conducted into labeling and tracking cells with the use of ^{19}F MRI. The PFCs used in research show to have only minor side effects on the cells[1, 2, 4-8, 23, 33, 37] and the fundamentally different way of imaging compared to paramagnetic agents, provides the possibility to trace these compounds very selectively *in vivo*. Currently, the commercially available CS-1000 is already approved for the use in a phase I clinical trial. But before ^{19}F imaging can be clinically applied a lot of research still has to be conducted. Optimization of sensitivity and imaging protocols should be developed before translation into the clinic is possible. However, ^{19}F imaging of cells in *vivo* is a promising technique that could enable quick, non-invasive way of analyzing the damaged regions in the brain after a brain injury and thereby provide fast, more effective and more personalized medicine to patients.[26]

9. References

[1] J. G. Riess, *Artificial Cells Blood Substitutes and Biotechnology* **2006**, *34*, 567.
[2] D. R. Spahn, *Critical Care* **1999**, *3*, R93.
[3] M. Krafft, *Advanced Drug Delivery Reviews* **2001**, *47*, 209.
[4] J. G. Riess, *Artificial Cells Blood Substitutes and Biotechnology* **2005**, *33*, 47.
[5] M. P. Krafft, J. G. Riess, *Biochimie* **1998**, *80*, 489.
[6] J. M. Janjic, E. T. Ahrens, *Wiley Interdisciplinary Reviews-Nanomedicine and Nanobiotechnology* **2009**, *1*, 492.
[7] J. G. Riess, *Chemical Reviews* **2001**, *101*, 2797.
[8] J. G. Riess, *Tetrahedron* **2002**, *58*, 4113.
[9] J. Chen, L. G.M., S. A. Wickline, *WIREs Nanomed Nanobiotechnology* **2010**, *2*, 431.
[10] F. Bonetto, M. Srinivas, A. Heerschap, R. Mailliard, E. T. Ahrens, C. G. Figdor, I. J. M. de Vries, *International Journal of Cancer* **2011**, *129*, 365.
[11] I. Celsense, (Ed.: I. Celsense), Pittsburg, **2010**.
[12] W. Wolf, C. A. Presant, V. Walluch, *Advanced Drug Delivery Reviews* **2000**, *41*, 55.
[13] G. Holland, P. Bottomley, W. Hinshaw, *Journal of Magnetic Resonance* **1977**, *28*, 133.
[14] E. T. Ahrens, R. Flores, H. Y. Xu, P. A. Morel, *Nature Biotechnology* **2005**, *23*, 983.
[15] P. Boehm-Sturm, L. Mengler, S. Wecker, M. Hoehn, T. Kallur, *Plos One* **2011**, *6*, e29040.
[16] S. D. Caruthers, A. M. Neubauer, F. D. Hockett, R. Lamerichs, P. M. Winter, M. J. Scott, P. J. Gaffney, S. A. Wickline, G. M. Lanza, *Investigative Radiology* **2006**, *41*, 305.
[17] I. Celsense, Celsense, Inc, Pittsburg, **2009**.
[18] U. Flogel, Z. Ding, H. Hardung, S. Jander, G. Reichmann, C. Jacoby, R. Schubert, J. Schrader, *Circulation* **2008**, *118*, 140.
[19] B. M. Helfer, A. Balducci, A. D. Nelson, J. M. Janjic, R. R. Gil, P. Kalinski, I. J. M. De Vries, E. T. Ahrens, R. B. Mailliard, *Cytotherapy*, *12*, 238.
[20] U. Himmelreich, T. Dresselaers, *Methods* **2009**, *48*, 112.
[21] U. Himmelreich, M. Hoehn, *Minimally Invasive Therapy & Allied Technologies* **2008**, *17*, 132.
[22] T. K. Hitchens, Q. Ye, D. F. Eytan, J. M. Janjic, E. T. Ahrens, C. Ho, *Magnetic Resonance in Medicine* **2011**, *65*, 1145.
[23] J. M. Janjic, M. Srinivas, D. K. K. Kadayakkara, E. T. Ahrens, *Journal of the American Chemical Society* **2008**, *130*, 2832.
[24] M. P. Krafft, J. G. Riess, *Journal of Polymer Science Part a-Polymer Chemistry* **2007**, *45*, 1185.
[25] G. M. Lanza, K. D. Wallace, M. J. Scott, W. P. Cacheris, D. R. Abendschein, D. H. Christy, A. M. Sharkey, J. G. Miller, P. J. Gaffney, S. A. Wickline, *Circulation* **1996**, *94*, 3334.

[26] G. M. Lanza, P. M. Winter, A. M. Neubauer, S. D. Caruthers, F. D. Hockett, S. A. Wickline, *Current Topics in Developmental Biology, Volume 70* **2005**, *70*, 57.
[27] K. C. Partlow, J. J. Chen, J. A. Brant, A. M. Neubauer, T. E. Meyerrose, M. H. Creer, J. A. Nolta, S. D. Caruthers, G. M. Lanza, S. A. Wickline, *Faseb Journal* **2007**, *21*, 1647.
[28] J. Ruiz-Cabello, B. P. Barnett, P. A. Bottomley, J. W. M. Bulte, *Nmr in Biomedicine* **2010**, *24*, 114.
[29] J. Ruiz-Cabello, P. Walczak, D. A. Kedziorek, V. P. Chacko, A. H. Schmieder, S. A. Wickline, G. M. Lanza, J. W. M. Bulte, *Magnetic Resonance in Medicine* **2008**, *60*, 1506.
[30] L. Shan, in *Molecular Imaging & Contrast Agent Database*, NIH, **2011**.
[31] E. M. Shapiro, K. Sharer, S. Skrtic, A. P. Koretsky, *Magnetic Resonance in Medicine* **2006**, *55*, 242.
[32] R. Southworth, M. Kaneda, J. J. Chen, L. Zhang, H. Y. Zhang, X. X. Yang, R. Razavi, G. Lanza, S. A. Wickline, *Nanomedicine-Nanotechnology Biology and Medicine* **2009**, *5*, 359.
[33] M. Srinivas, E. Aarntzen, J. W. M. Bulte, W. J. Oyen, A. Heerschap, I. J. M. de Vries, C. G. Figdor, *Advanced Drug Delivery Reviews*, *62*, 1080.
[34] M. Srinivas, L. J. Cruz, F. Bonetto, A. Heerschap, C. G. Figdor, I. J. M. de Vries, *Biomaterials* **2010**, *31*, 7070.
[35] M. Srinivas, A. Heerschap, E. T. Ahrens, C. G. Figdor, I. J. M. de Vries, *Trends in Biotechnology* **2010**, *28*, 363.
[36] M. Srinivas, P. A. Morel, L. A. Ernst, D. H. Laidlaw, E. T. Ahrens, *Magnetic Resonance in Medicine* **2007**, *58*, 725.
[37] M. Srinivas, M. S. Turner, J. M. Janjic, P. A. Morel, D. H. Laidlaw, E. T. Ahrens, *Magnetic Resonance in Medicine* **2009**, *62*, 747.
[38] E. A. Waters, J. J. Chen, J. S. Allen, H. Y. Zhang, G. M. Lanza, S. A. Wickline, *Journal of Cardiovascular Magnetic Resonance* **2008**, *10*, 9.
[39] E. A. Waters, J. J. Chen, X. X. Yang, H. Y. Zhang, R. Neumann, A. Santeford, J. Arbeit, G. M. Lanza, S. A. Wickline, *Magnetic Resonance in Medicine* **2008**, *60*, 1232.
[40] G. Weise, T. C. Basse-Luesebrink, C. Wessig, P. M. Jakob, G. Stoll, *Experimental Neurology* **2011**, *229*, 494.
[41] G. Weise, T. C. Basse-Lusebrink, C. Kleinschnitz, T. Kampf, P. M. Jakob, G. Stoll, *Plos One* **2011**, *6*, 8.
[42] R. M. Winslow, Elsevier Inc., London, **2006**.
[43] H. Y. Zhang, in *Molecular Imaging & Contrast Agent Database*, NIH, **2008**.
[44] H. Y. Zhang, in *Molecular Imaging & Contrast Agent Database*, NIH, **2008**.
[45] A. Bondi, *Journal of Physical Chemistry* **1964**, *68*, 441.
[46] D. E. Williams, D. J. Houpt, *Acta Crystallographica Section B-Structural Science* **1986**, *42*, 286.
[47] D. Simberg, R. Mattrey, *Journal of Drug Targeting* **2009**, *17*, 392.
[48] D. J. Smith, E. S. Kornbrust, T. A. Lane, *Artificial Cells Blood Substitutes and Immobilization Biotechnology* **1994**, *22*, 1215.
[49] R. F. Mattrey, D. M. Long, F. Multer, R. Mitten, C. B. Higgins, *Radiology* **1982**, *145*, 755.
[50] A. Ratner, R. Hurd, H. Muller, B. Bradley-Simpson, W. Pitts, *1987* **1987**, *5*, 548.

[51] Philips, *Basic Principles of MR Imaging*, Eindhoven.
[52] R. Wechselberger, Utrecht University (Utrecht), **2007**.
[53] CambridgeSoft, 12.0 ed., Cambridge, **2009**.
[54] J. K. Hsiao, M. F. Tai, H. H. Chu, S. T. Chen, H. Li, D. M. Lai, S. T. Hsieh, J. L. Wang, H. M. Liu, *Magnetic Resonance in Medicine* **2007**, *58*, 717.
[55] C. Heyn, C. V. Bowen, B. K. Rutt, P. J. Foster, *Magnetic Resonance in Medicine* **2005**, *53*, 312.
[56] D. Delli Castelli, E. Gianolio, S. Geninatti Crich, E. Terreno, S. Aime, *Coordination Chemistry Reviews* **2008**, *252*, 2424.
[57] B. M. Kok, S. Hak, J. M. Mulder, D. W. J. van der Schaft, G. J. Strijkers, K. Nicolay, *Magnetic Resonance in Medicine* **2009**, *61*, 1022.
[58] J. W. M. Bulte, *Nature Biotechnology* **2005**, *23*, 945.
[59] A. M. Morawski, P. M. Winter, X. Yu, R. W. Fuhrhop, M. J. Scott, F. Hockett, J. D. Robertson, P. J. Gaffney, G. M. Lanza, S. A. Wickline, *Magnetic Resonance in Medicine* **2004**, *52*, 1255.
[60] J. N. Marsh, K. C. Partlow, D. R. Abendschein, M. J. Scott, G. M. Lanza, S. A. Wickline, *Ultrasound in Medicine and Biology* **2007**, *33*, 950.
[61] K. C. Lowe, *Tissue Engineering* **2003**, *9*, 389.
[62] A. M. Neubauer, J. Myerson, S. D. Caruthers, F. D. Hockett, P. M. Winter, J. J. Chen, P. J. Gaffney, J. D. Robertson, G. M. Lanza, S. A. Wickline, *Magnetic Resonance in Medicine* **2008**, *60*, 1066.
[63] P. M. Winter, S. D. Caruthers, A. Kassner, T. D. Harris, L. K. Chinen, J. S. Allen, *Cancer Research* **2003**, *63*, 5838.
[64] M. G. Freire, A. M. A. Dias, M. A. Z. Coelho, J. A. P. Coutinho, I. M. Marrucho, *Journal of Colloid and Interface Science* **2005**, *286*, 224.
[65] M. Postel, J. G. Riess, J. G. Weers, *Artificial Cells Blood Substitutes and Immobilization Biotechnology* **1994**, *22*, 991.
[66] A. S. Kabalnov, E. D. Shchukin, *Advances in Colloid and Interface Science* **1992**, *38*, 69.
[67] S. M. I. Group, Softways, **2003-2012**.
[68] H. Lee, R. R. Price, G. E. Holburn, C. L. Partain, M. D. Adams, W. P. Cacheris, *Jmri-Journal of Magnetic Resonance Imaging* **1994**, *4*, 609.
[69] S. R. Thomas, R. G. Pratt, R. W. Millard, R. C. Samaratunga, Y. Shiferaw, L. C. Clark Jr, R. E. Hoffmann, *Journal of Magnetic Resonance Imaging* **1994**, *4*, 631.
[70] S. Flacke, S. Fischer, M. J. Scott, R. W. Fuhrhop, J. S. Allen, M. McLean, P. M. Winter, G. A. Sicard, P. J. Gaffney, S. A. Wickline, G. M. Lanza, *Circulation* **2001**, *104*, 1280.
[71] P. M. Winter, A. M. Morawski, S. D. Caruthers, R. W. Fuhrhop, H. Y. Zhang, T. A. Williams, J. S. Allen, E. K. Lacy, J. D. Robertson, G. M. lanza, S. A. Wickline, *Circulation* **2003**, *53*, 621.
[72] Q. Ye, D. Yang, M. Williams, D. S. Williams, C. Pluempitiwiriyawej, J. M. Moura, C. Ho, *Kidney International* **2002**, *61*, 1124.